Solubility-pH profile of desipramine hydrochloride in saline phosphate buffer: Enhanced solubility due to drug-buffer aggregates

Olivera S. Marković, Miloš P. Pešić, Ankita V. Shah, Abu T.M. Serajuddin, Tatjana Ž. Verbić, Alex Avdeef

PII: S0928-0987(19)30117-4
DOI: https://doi.org/10.1016/j.ejps.2019.03.014
Reference: PHASCI 4880

To appear in: *European Journal of Pharmaceutical Sciences*

Received date: 23 January 2019
Revised date: 22 February 2019
Accepted date: 18 March 2019

Please cite this article as: O.S. Marković, M.P. Pešić, A.V. Shah, et al., Solubility-pH profile of desipramine hydrochloride in saline phosphate buffer: Enhanced solubility due to drug-buffer aggregates, European Journal of Pharmaceutical Sciences, https://doi.org/10.1016/j.ejps.2019.03.014

Solubility-pH profile of desipramine hydrochloride in saline phosphate buffer: enhanced solubility due to drug-buffer aggregates

Olivera S. Marković[a], Miloš P. Pešić[b], Ankita V. Shah[c,d], Abu T. M. Serajuddin[c], Tatjana Ž. Verbić[b,*], Alex Avdeef[e,*]

[a]Department of Chemistry – IChTM, University of Belgrade, Njegoševa 12, 11000 Belgrade, Serbia (olivera.markovic@ihtm.bg.ac.rs)

[b]University of Belgrade – Faculty of Chemistry, Studentski trg 12-16, 11000 Belgrade, Serbia (mpesic@chem.bg.ac.rs; tatjanad@chem.bg.ac.rs)

[c]St. John's University, College of Pharmacy and Health Sciences, 8000 Utopia Parkway, Queens, NY 11439, USA (serajuda@stjohns.edu)

[d]Current address: Freund-Vector Corporation, 675 44th Street, Marion, IA 52402 (Ankita.Shah@freund-vector.com)

[e]*in-ADME* Research, 1732 First Avenue #102, New York, NY 10128, USA (alex@in-ADME.com).

[*]Corresponding authors: tatjanad@chem.bg.ac.rs, alex@in-adme.com

ABSTRACT

Although solubility-pH data for desipramine hydrochloride (DsHCl) have been reported previously, the aim of the present study was to critically examine the aqueous solubility-pH behavior of DsHCl in buffer-free and buffered solutions, in the presence of physiologically-relevant chloride concentration, using experimental practices recommended in the recently-published "white paper" (Avdeef et al., 2016). The computer program *p*DISOL-X was used to design the structured experiments (pH-RSF method), to process the data, and to refine the equilibrium constants. Low-to-high and high-to-low pH assays (using HCl, H_3PO_4, or NaOH to adjust pH) were performed on phosphate-buffered (0.12-0.15 M) saturated solutions of DsHCl in the pH 1.3-11.6 range. After equilibration (stirring 6 h, followed by 18 h stir-free sedimentation), filtration or centrifugation was used for phase separation. Concentration was measured using HPLC with UV/VIS detection. The 2:1 drug-phosphate solubility product ($K_{sp}^{2:1} = [DsH^+]^2[HPO_4^{2-}]$) was determined from data in the pH 4-9 region. The free base of desipramine was prepared and used to determine the $K_{sp}^{1:1}$ ($[DsH^+][H_2PO_4^-]$) in chloride-free acidified suspension. In addition, phosphate-free titrations were conducted to determine the intrinsic solubility, S_0, and the 1:1 drug-chloride solubility product, $K_{sp}^{DsH.Cl} = [DsH^+][Cl^-]$. Under the assay conditions, only the phosphate-free solutions showed some supersaturation near pH_{max} 8.0. In phosphate-containing solutions, pH_{max} was indicated at higher pH (8.8-9.6). Oils mixed with solids were observed to form in alkaline solutions (pH > 11). Notably, soluble drug-phosphate *complexes* appeared to form below pH 3.9 and above pH_{max} in saturated phosphate-containing saline solutions. This was indicated by the systematic pH shift to higher values in the log *S*-pH curve in alkaline solution than expected from the Henderson-Hasselbalch equation. For pH < 3.9, saturated phosphate-containing saline solutions exhibited elevated solubility, with drug-*hydrochloride* as the sole precipitate. Salt solubility products, intrinsic solubility, and complexation constants, which rationalized the data, were determined. Elemental, thermogravimetric (TGA), differential scanning calorimetric (DSC), and powder X-ray diffraction (PXRD) analyses were used to characterize the precipitates isolated from suspensions at different pH.

Keywords: desipramine-phosphate complexes; pH effect; buffer effect; solubility product; pH-Ramp Shake-Flask method; *p*DISOL-X.

1. Introduction

Amphiphilic tricyclic bases, such as dibenzazepines and phenothiazines, are surface-active, sparingly-soluble drugs, which can exhibit complicated aqueous solution chemistry. Many of the drugs in free-base form have low melting points (Bradley *et al*., 2018). In highly alkaline solutions, these drugs sometimes separate out of solution as oil, with elevated solubility. Surface-active drugs often form supersaturated solutions near the salt-to-free-base transition pH (pH_{max}), where partially-charged sub-micellar or micellar aggregates form (Higuchi *et al.*, 1953; Zografi *et al.*, 1964; Zografi and Zarenda, 1966; Sorby *et al.*, 1966; Green, 1967; Florence and Parfitt, 1971; Attwood *et al*., 1974; Liu and Hurwitz, 1977; Bogardus and Blackwood, 1979; Serajuddin and Rosoff, 1984; Serajuddin and Jarowski, 1985; Fini *et al.*, 1995; Zhu and Streng, 1996; Attwood *et al.*, 1997; Ledwidge and Corrigan, 1998; Gebauer *et al.*, 2014).

The above drugs precipitate over a wide range of pH, forming solids in contact with dissolved monomers, and often, also with water-soluble sub-micellar aggregates (*e.g*., dimers, trimers, and higher-order oligomers). Attwood *et al.* (1974) found that distilled water solutions of promazine and chlorpromazine hydrochlorides form small micelles in aggregated units of eleven monomers. Zografi and Zarenda (1966) noted that a 2-5 μM (below solubility limit) solution prepared from chlorpromazine *free base* (pH 9-12) showed no surface activity. However, a 30 μM *hydrochloride* solution at pH 9 produced a stable supersaturated solution, which partly separated as oil (liquid-liquid phase separation, LLPS) and was more soluble than the crystalline free base. The above operationally non-commutative solubility behavior may be further influenced by complexation/hydrotropy reactions, depending on the buffer used (Shoghi *et al*., 2013).

The earliest measurement of the intrinsic solubility (S_0) of desipramine appears to be that of Green (1967), who reported log S_0 = -3.66. More recently, a buffer-free potentiometric method was used to determine the intrinsic solubility of desipramine as log S_0 = -3.81 (Bergström *et al*., 2003). Also, both the log S_0 -3.69 and the pK_a 10.28 values were *simultaneously* determined using the *p*SOL (Pion Inc.) buffer-free method (Avdeef, 2012). A small-scale shake-flask solubility measurement of desipramine hydrochloride in the pH range of 1.4 to11.2 in 0.15 M phosphate solution revealed a curve that did not adhere to the shape predicted by the simple Henderson-Hasselbalch (HH) equation (Bergström *et al*., 2004). When the HH equation was applied to the point at pH 11.2, log S_0 = -3.90. On the other hand, a sigmoidal fit of the data in the alkaline region suggested log S_0 = -3.37. The observed log *S*-pH slope in the diagonal region was reported as -0.6, whereas -1 would have been expected from the HH equation. Since the lower inflection in the fitted curve was near pH 7.5, well below the pK_a, an alternative model based on putative aggregation of the free base indicated log S_0 = -6.40 (Avdeef, 2014b), a value very

different from those of all the other studies. Solid state characterizations to identify the solids isolated from suspensions at various pH were not reported in the above studies. The solution behavior of desipramine in phosphate-buffered and unbuffered solutions is evidently complicated and only tentatively understood, given the above incongruities.

The aim of the present study was to critically re-examine the aqueous solubility-pH behavior of desipramine hydrochloride (DsHCl) in phosphate-buffered and buffer-free solutions, in the presence of physiologically-relevant chloride concentration. Specifically, solubility was measured: (a) using state-of-the-art experimental design, as recommended in a "white paper" on solubility (Avdeef *et al.*, 2016), drawing on expert consensus opinions from researchers in six countries; (b) performing solubility titrations in two directions, pH 11.6→1.3 as well as 1.3→11.6; (c) using both DsHCl and Ds (free base), as starting solids; (d) performing titrations in chloride-containing media, without any phosphate; (e) performing the converse measurements (phosphate-containing, chloride-free media); (f) isolating solids at critical log *S*-pH points and performing solid state characterizations using elemental, thermogravimetric, differential scanning calorimetric, and powder X-ray diffraction analyses. The recently-developed computational methods were applied to determine aggregation and/or complexation constants and stoichiometries from solubility-pH data (Avdeef, 2007, 2012; Völgyi *et al.*, 2013; Avdeef, 2014a,b; Butcher *et al.*, 2015; Pobudkowska *et al*., 2016; Takács-Novák *et al*., 2017). We sought to determine the solubility products $K_{sp}^{1:1}$ ($[DsH^+][H_2PO_4^-]$), $K_{sp}^{2:1}$ ($[DsH^+]^2[HPO_4^{2-}]$), $K_{sp}^{DsH.Cl}$ ($[DsH^+][Cl^-]$), as well as S_0. We anticipated to find evidence of drug aggregates (e.g., $(DsH^+)_n$ or $(DsH^+.Ds)_n$) , but instead found drug-phosphate *complexes* forming below pH 4 and above pH_{max} in saturated phosphate-containing saline solutions.

2. Materials and methods

2.1 Chemicals and reagents

Desipramine hydrochloride (DsHCl) and sodium dihydrogen phosphate dihydrate (analytical reagent grade) were purchased from Sigma-Aldrich and used as received. Hydrochloric acid and sodium hydroxide were purchased from Merck (Titrisol® ampoules). Phosphoric acid (analytical reagent grade) was purchased from Fisher Chemical. All solutions were prepared with Millipore-purified water.

2.2 pH *measurement*

In all experiments, pH values were measured using Crison pH-Burette 24 2S equipped with a

micro-combined pH electrode (Crison pH electrode 50 29). The electrode was calibrated by standard Crison buffer solutions (pH 4.01, 7.00, and 9.21).

2.3 HPLC concentration determination

After equilibration in the solubility experiments, excess solid was removed by filtration or centrifugation (cf., Supplementary Material). The concentration of the drug in the supernatant was determined by HPLC-UV/VIS system (Agilent Technologies 1260 Infinity LC System). Chromatographic separation was conducted using Zorbax Eclipse XDB-C18 50×4.6 mm column with 1.8 µm particles at flow rate of 0.5 mL/min. Gradient elution was used: from 70% A + 30% B to 100% B during 5 minutes, 100% B for 1 minute, and back to 70% A + 30% B during 1 minute (solvent A: water with 1% acetic acid; solvent B: acetonitrile). Detection wavelength: 250 nm; column temperature: 25°C.

2.4 Differential scanning calorimetric (DSC) analysis

Solids isolated from suspensions were analyzed for their thermal behavior as a function of temperature using a Q200 differential scanning calorimeter (TA instruments, DE, USA). Samples (5-10 mg each) were sealed in Tzero pan with a pinhole for the escape of any volatile material. The samples were equilibrated at 5°C for 5 min and then heated at the rate of 10°C/min to the final temperature of ~225°C that was above the potential melting points of samples. When heat-cool-heat cycles were used, samples were prepared similarly and then initial heating, cooling and reheating were conducted at rates of 10, 30 and 3°C; the reheating was done at a lower heating rate to facilitate any recrystallization of material. The results were analysed using Universal Analysis software version 2000 (TA Instruments).

2.5 Thermogravimetric Analysis (TGA)

Approximately 4-6 mg of samples were analyzed using the TGA Q50 thermogravimetric analyzer, (TA instruments, DE, USA). The samples were heated from ~25°C to 300°C at a heating rate of 10°C/min in a nitrogen environment.

2.6 Powder X-ray diffraction (PXRD) analysis

A powder X-ray diffractometer (Shimadzu 6000, Kyoto, Japan) was used to obtain PXRD patterns at room temperature with a monochromatic CuKα radiation source operated at 40 kV and 30 mA

and the scanning rate of 2°/min over the 2θ range of 10° to 60°. The test materials were placed as thin layers inside glass sample holders.

2.7 Elemental analysis

The elemental analysis was accomplished by combustion analysis on a Vario EL III C,H,N,S/O Elemental Analyzer (Elementar Analysensysteme GmbH, Hanau-Germany).

2.8 Solubility determination using the pH-*Ramp Shake-Flask (*pH-*RSF) method*

Before commencing any assays, solubility-pH simulations were performed using the computer program *p*DISOL-X™ (*in-ADME* Research). This was to plan for the weights of reagents to use (including buffers, if suggested), as well as the expected volumes of titrants to add in order to adjust the pH to suitable spacing (e.g., 0.2-0.5 units) across the whole pH range of interest. Knowledge of the drug pK_a value and an *in silico* estimate of the intrinsic solubility, S_0, are essential. Also, in the case of phosphate-containing media, drug-phosphate solubility products (K_{sp}) can be approximated from the S_0 values (Avdeef, 2014b). For other counterions, the *sdiff* 3-4 approximation (Avdeef *et al*., 2000) may be used if the ionic strength is near ~0.15 M. The pK_a values of most common buffers, as a function of temperature and ionic strength, are encoded in the computer program used to design assay. Ordinarily, buffers are only recommended when pH adjustment cannot be precisely controlled by additions of standardized strong acid (e.g., HCl) or strong base (e.g., NaOH) titrant. The conversion of pH electrode reading from the "operational" scale to the concentration scale was effected by a four- parameter calibration procedure (Avdeef and Bucher, 1978; Avdeef, 2012). The experiments conducted here were guided by the above ("think-before-leap") procedure, which we call the pH-Ramp Shake-Flask (pH-RSF) method.

By contrast, traditional procedures are often trial-and-error in staging the collection of data. A series of buffers is selected to cover a range of pH suitable for the study. Phosphate, acetate, and borate buffers are commonly selected, often at 50-100 mM concentration. Solid compound is added incrementally to a solution buffered at a desired pH until an unspecified "excess" solid remains undissolved. In some cases, the procedure significantly alters the initial pH of the solution, requiring adjustments by additions of a strong acid or base. Sometimes, the buffer constituents form complexes with the drug (Shoghi *et al*., 2013), *raising* the equilibrium solubility. Also, buffer constituents may act as counterions leading to drug-salt precipitation, *lowering* the equilibrium solubility. Some buffers interfere with the analytical methods used to determine drug concentration (e.g., phosphate buffers in mass spectrometry). Assay details are often inadequately documented in traditional studies.

Tables S1-S3 given in Supplementary material summarize in sufficient detail the initial compositions and experimental conditions used in the solubility experiments. The temperature was kept constant at 25±1°C. Titrant solutions of HCl, NaOH, and H_3PO_4 were nominally 1 M, with precise concentrations determined potentiometrically.

2.8.1 Sets 1 and 2 (high-to-low pH *titration replicates)*

Titrations were performed in two directions: high-to-low pH values (Sets 1 and 2) and low-to-high pH (Set 3). Sets 1 and 2: *alkaline* stock solutions were prepared by mixing 39.5 mL of 0.15 M NaH_2PO_4 (pH 4.34-4.37) and 10.5 mL standardized 1 M NaOH. DsHCl was added directly to the stock solutions: 0.41170 g (Set 1) and 0.41220 g (Set 2). Two-milliliter aliquots of the *well-mixed* drug-containing saturated stock suspensions were placed into each of 13 vials. The initial pH in the vials was 11.5-11.6. To each vial, a pre-calculated different volume of standardized 1 M HCl was added, ranging from 0 to 410 μL. The vials were capped and stirred for 6 h. After that, stirring was turned off, and sedimentation was allowed to take place for a further 18 h ("6+18 h" agitation-sedimentation equilibration sequence suggested in the "white paper"). All solids in the suspensions dissolved below pH 4.

2.8.2 Set 3 (low-to-high pH *titration)*

The Set 3 *acidic* stock solution was prepared by mixing 14.0 mL of 0.15 M NaH_2PO_4 (pH 4.45) and 1.00 mL standardized 1 M HCl. To the stock solution, 0.34370 g of DsHCl was added. A 1-mL aliquot of the *well-mixed* stock suspension was placed into each of 11 vials. To each vial, a different volume of standardized 1 M NaOH was added, ranging from 80 to 370 μL. The vials were capped and agitated as before ("6+18 h"). Below pH 4, no solids were found to precipitate in the vials.

2.8.3 Set 4 (raised concentrations)

Set 4 was designed to force precipitation in the pH 2-4 region. In the experiments, 0.900 mL of 0.15 M NaH_2PO_4 solution was added to each of three vials containing 0.08650-0.08730 g DsHCl. The pH was adjusted using 1 M H_3PO_4 (Samples 1 and 2), NaOH (Sample 2), or HCl (Sample 3). The vials were capped and the solutions were allowed to equilibrate as before ("6+18 h"). Phases were separated by centrifugation (Samples 1 and 2) or filtration (Sample 3).

2.8.4 Set 5 (phosphate-free titrations)

A set without phosphate buffer was also designed (Set 5) in order to determine the drug-hydrochloride solubility product in phosphate-free suspensions. Precisely 1.00 mL of 0.15 M NaCl was added to each of 7 vials containing accurately-weighed 0.04745-0.11205 g of DsHCl. The pH was

adjusted with standardized HCl (1.0211 M) and/or standardized NaOH (1.0215 M). Stirring was followed by sedimentation ("6+18 h"). Equilibrated pH values ranged from 1.31 to 10.04. Phases were separated by centrifugation.

The detailed titration and solubility data are summarized in **Tables S4-S8** (Supplementary Material).

2.9 Preparation of samples for solid state characterization

The above five titration sets did not produce sufficient amounts of solid for further analysis. So, in order to characterize the solid precipitate found in samples after equilibration, two series of additional experiments (below) were performed at pH expected to contain a specific *single* solid form of the drug, as suggested by preliminary analyses of the above five titration sets.

2.9.1 Series 1 (Samples OM11-OM15, from suspensions containing both chloride and phosphate)

Precisely 2.00 mL of 0.15 M NaH_2PO_4 solution were added to 5 vials containing accurately weighted 0.14-0.18 g of DsHCl. The total drug concentrations were about 2-3 times higher than those of Set 3. The pH was adjusted with 1 M HCl or NaOH. The vials were capped and allowed to equilibrate ("6+18 h"). Phases were separated by centrifugation, and each solid was further analyzed. The assay design details are summarized in **Table S2** (Supplementary Material).

2.9.2 Series 2 (Samples OM21-OM25, with one solid isolated from chloride-free suspensions)

Sample OM21 was prepared in two steps. (a) To isolate the free base: precisely 2.00 mL of 0.15 M NaH_2PO_4 solution were added to 0.125 g of DsHCl and mixed with 650 µL of 1 M NaOH. The sample was stirred for 6 h and left to sediment for 62 h. Despite longer sedimentation time at pH 11.6, precipitate was still oily. Phases were separated by centrifugation. Solid Ds (free base) was left to dry. (b) 900 µL of 0.15 M NaH_2PO_4 solution were added to 0.096 g of Ds precipitate from step (a) and mixed with 400 µL of 1 M H_3PO_4. The low-pH suspension was allowed to equilibrate ("6+18 h"). Phases were separated by centrifugation. The OM21 solid was washed with purified water and left to dry.

Samples OM22-OM25 approximately paralleled the compositions in Set 3, except that 2-3 times higher drug concentrations were used. The specific quantities of reagents used are summarized in **Table S3** (Supplementary Material). Equilibration followed the "6+18 h" procedure. The solids were separated from the suspensions by centrifugation, washed with purified water, and allowed to dry in air.

2.10 Refinement of intrinsic and salt solubility, aggregation and complexation constants

The mathematical approach used in the *p*DISOL-X log *S*-pH simulation-refinement has been described by Völgyi *et al.* (2013). The program has been applied in several other recent studies (Avdeef, 2014a, b; Butcher *et al.*, 2015; Avdeef, 2015; Pobudkowska *et al*., 2016; Takács-Novák *et al.*, 2017). Briefly, the data analysis method uses log *S*-pH as measured input data, with concentrations determined by a suitable analytical technique. The analytical concentrations of all added reagents are specified. "Excess drug added" is not sufficient information when drug-phosphate salts are suspected to precipitate during the titration, as emphasized in the "white paper." The mass action algorithm considers the contribution of all species proposed to be present in solution, including all buffer, counterion, and inert electrolyte components. The approach does not assume the validity of the Henderson-Hasselbalch relationship, nor does it depend on any explicitly derived extensions of the HH equations. The mass action algorithm derives its own implicit equations internally, given any practical number of hypothesized equilibrium reactions and the corresponding estimated constants, which are subsequently refined by weighted nonlinear least-squares regression. The presence of specific drug-phosphate precipitates can be tested. The program calculates the distribution of species consequent to a sequence of additions of standardized strong-acid titrant HCl (or ionizable-acid titrants such as H_3PO_4) to simulate the suspension pH-speciation down to pH ~ 0, the staging point for the subsequent steps. Then, a sequence of perturbations with standardized strong-base titrant (e.g., NaOH) is simulated, and solubility calculated at each point, until pH ~ 13 is reached. The ionic strength, I, is rigorously calculated at each step, and the pK_a value (as well as solubility products, aggregation and complexation constants), along with pH electrode calibration constants, are accordingly adjusted for changes from the benchmark level of 0.15 M (Avdeef, 1992, 2012).

At the end of the pH-speciation simulation, the calculated log *S*- pH curve is compared to measured log *S* vs. pH. A user-supervised log *S*-weighted nonlinear least squares refinement commences to refine the user-proposed equilibrium model. The underlying differential equations are solved using analytical expressions encoded in the program. The process is repeated until the differences between calculated and measured log *S* values reach a minimum. Different model species are tested to make further improvements in the fit.

3. Results and discussion

3.1 Summary of the interlaboratory consensus recommendations applied in this study

The "white paper" commentary (Avdeef *et al.*, 2016) reviewed a number of factors that can affect the quality of equilibrium solubility measurement as a function of pH of sparingly-soluble druglike molecules. It was asserted that the traditional shake-flask method is the "gold standard," although other validated methods with well-defined protocols could also be used. It was stressed that *independently-determined* pK_a values of the drug be used in the analysis of the log *S*-pH data. The importance of solid state characterization was also stressed, citing several case studies of polymorphic transformations. The complexity on the solution side of solubility-pH measurement was illustrated with several case studies, where aggregates (micellar and sub-micellar) and drug-buffer complexes appeared to form. The importance of measuring the *final* pH (not that of the starting buffer) accurately in buffered and unbuffered solutions was discussed at length. Methods and pitfalls of separating solid from saturated solutions were critically discussed. The reporting of the temperature, ionic strength, buffer compositions, and other experimental detail was encouraged. When such "good practices" could be followed, it was expected that high quality results in solubility measurement could be achieved.

3.2 pK_a *determination from solubility*-pH *data*

The independently measured pK_a of desipramine, 10.28 ± 0.03 (26°C, I_{ref} 0.15 M), verified by three different potentiometric procedures (Avdeef, 2012), was used in the study here. The apparent constant determined from the current log *S*-pH data led to values as high as 10.44. The significant difference between the two values led us to suspect that either aggregation or complexation reactions may be present in the phosphate-containing alkaline solutions.

3.3 Solubility analysis

3.3.1 Data

The solubility-pH profiles of DsHCl in buffer-free and phosphate buffer, designed with the pH-RSF method, are shown in **Figure 1.** The reported solubility values are based on molarity units. The detailed titration ($V_{titrant}$- pH) and solubility (log *S*-pH) data are presented in **Tables S4-S10** (Supplementary Material).

Sets 1 and 2 (**Figure 1a**) are duplicate experiments, where alkaline suspensions (pH 11.6)

containing $[Ds]_{tot} = [Cl]_{tot}$ = 27 mM and $[PO_4]_{tot}$ = 119 mM, were acidified with HCl. Set 3 (**Figure 1b**) represents the titration in the opposite direction, where acidified (pH 1.90) suspensions, with somewhat higher concentrations $[Ds]_{tot}$ = 76 mM, $[Cl]_{tot}$ = 142 mM, and $[PO_4]_{tot}$ = 140 mM, were titrated with NaOH up to pH 11.6. In the three sets, solutions below pH 3.9 did not achieve saturation.

Set 4 (upper **Figure 1c**) was designed in order to get solid precipitate in pH region below 4. Higher drug concentrations were used: $[Ds]_{tot} = [Cl]_{tot}$ = 320 and $[PO_4]_{tot}$ = 150 mM. The number of analysed samples in this pH region was limited due to excessive amounts of DsHCl required to reach saturation.

Due to the possibility of co-precipitation of chloride and phosphate drug salts at low pH (Völgyi *et al.*, 2013), the phosphate-free Set 5 (lower **Figure 1c**) experiments were designed to determine the $K_{sp}^{DsH.Cl} = [DsH^+][Cl^-]$, without interference from phosphate. $[Ds]_{tot}$ ranged from 145 to 369 mM and $[Cl]_{tot}$ from 145 to 402 mM (*cf.*, **Table S8**).

Series 1 and 2 measurements (*cf.*, **Tables S2**, **S3**, **S9**, and **S10**) were designed in order to get enough precipitate for solid state analysis.

3.3.2 Refinement of constants

Whereas the solubility product is an equilibrium constant, the solubility of a charged drug is variable, whose value depends on the concentration product of two independent reactants (drug and counterion). In the pH domain where the drug is charged, its solubility can be varied simply by selecting different concentrations of the counterion. The "common ion" effect of a drug hydrochloride salt is a good example of this phenomenon: the solubility of a positively-charged drug decreases as HCl is used to lower the pH (which increases the chloride counterion concentration).

The sample points from each of Sets 1-5 were designed (pH-RSF) specifically to be fit to a single log *S*-pH curve across a range of pH values, generally requiring that for each sample point, the total drug concentration (after correction for dilution) to be essentially the same, and that the drug:counterion ratio to be variable only when the titrant includes the counterion as a constituent. On the other hand, the Series 1 and 2 sets (Samples OM11-15 and OM21-25) were less constrained as they were designed to generate sufficient quantities of precipitate for solid state characterizations, with different samples possibly associated with different members of a conditional family of log *S*-pH curves.

The determination of equilibrium constants began with Sets 1 and 2 treated separately. Since nearly the same constants were determined by weighted nonlinear regression, the two sets were merged, and a combined analysis was performed. The refined constants are summarized in **Table 1** and the plot of the fitted curve is shown in **Figure 1a** by the solid curve. The dashed curve in the figure was calculated

with the Henderson-Hasselbalch (HH) equation, using the independently-determined pK_a 10.28. It is evident in **Figure 1a** for pH > pH_{max} (a conditional constant) that the points do not fall on the HH curve. In certain cases, the pK_a value can be determined from the solubility data. However, in our case the resultant value was significantly higher than the independently-determined pK_a. In complicated systems, it is not recommended that the pK_a value be determined from log *S*-pH data (Butcher *et al*., 2015; Völgyi *et al*., 2010). At least two possible explanations for the difference could be proposed here: (a) drug self-aggregation (e.g., dimer formation), or (b) drug-buffer complexation (e.g., Ds-phosphate anionic complexes). Since the analysis of Set 5 (lower **Figure 1c**) did not indicate deviations from the HH curve in the alkaline solution, drug-phosphate complexation (b) was favored over drug self-aggregation (a). The data were tested against several possible complexation reactions. The simplest which rationalized the data was based on the reaction involving the formation of a monoanionic complex,

$$Ds + DsH^+ + HPO_4^{2-} \leftrightarrows Ds(DsH^+)HPO_4^{2-} \quad (1a)$$

with the corresponding constant

$$\log K_{221} = [Ds(DsH^+)HPO_4^{2-}] / [Ds][DsH^+][HPO_4^{2-}] \quad (1b)$$

where the subscript 221 refers to the (Ds,H,PO_4) stoichiometry of the formed species. The refined value is log K_{221} = 4.58 ± 0.10 (**Table 1**). The pH 4-9 domain could be rationalized by the formation of the 2:1 drug salt,

$$(DsH^+)_2HPO_4^{2-}(s) \leftrightarrows 2\ DsH^+ + HPO_4^{2-} \quad (2a)$$

with the corresponding solubility product,

$$\log K_{sp}^{2:1} = [DsH^+]^2[HPO_4^{2-}] \quad (2b)$$

where the superscript 2:1 refers to the drug:phosphate stoichiometry of the formed solid. The refined value is log $K_{sp}^{2:1}$ = -7.38 ± 0.01 (**Table 1**).

Since the solutions in Set 1 and 2 contained chloride, it was necessary to verify that the solubility product was due solely to reaction (2a). Set 5, which contained no phosphate, indicated that the drug-chloride solubility product is log $K_{sp}^{DsH.Cl}$ = -2.19 ± 0.03 (**Table 1**). When this value was included in the equilibrium model for Sets 1 and 2, along with the other constants, it was found that the solubility product for the hydrochloride salt was not exceeded, so no hydrochloride salt co-precipitate was expected at the concentration levels in Sets 1 and 2 (pH > 4).

The intrinsic solubility, log S_0 = -3.85, was entered in the Sets 1 and 2 refinement as a fixed contribution, based on the value refined with the Set 5 data, which showed no deviations from the HH curve. It would be challenging to refine both the log S_0 and the log K_{221} simultaneously in Sets 1 and 2,

since the two constants are co-dependent.

Since the tendency to form a supersaturated solution (often near pH_{max}) depends on the solid state of the starting materials (e.g., Zografi and Zarenda, 1966), Set 3 was devised to be a titration going from low-to-high pH, in the direction opposite of that of Sets 1 and 2. **Figure 1b** shows the best-fit results of the analysis. In the alkaline solution of Set 3, there is comparable deviation from the HH curve, as in the case of Sets 1 and 2. **Table 1** lists the refined constants. The salt solubility was somewhat elevated in Set 3, compared to that in Sets 1 and 2. The complexation constants were slightly different, but not significantly, given the standard deviations, SD= 0.10, from the refinement in both cases. The measured solubility values of samples OM14, OM15, OM24 and OM25 were merged into the Set 3 calculations, since these OM samples were at $pH > pH_{max}$ (cf., **Figure 1b**), where salt precipitation is minimal. The OM samples were also consistent with complexation taking place.

As evident from the above discussion, the phosphate-free Set 5 data analysis played a key role in rationalizing the phosphate-containing model based on the Sets 1-3 data. Set 5 data were taken to be an accurate basis for the determination of the intrinsic solubility of desipramine: $\log S_0 = -3.85 \pm 0.04$, in the apparent absence of interference due to complex formation.

Set 4 (upper curve in **Figure 1c**) also played an important role in the evolution of the overall equilibrium model. The low pH and the high drug concentrations suggested that both DsH.Cl and $DsH.H_2PO_4$ could co-precipitate, since the $\log K_{sp}$, -2.19 (from Set 5) and -2.55 (from Sample OM21), respectively, were comparable. However, the inclusion of both constants in the data analysis could not explain the upper curve in **Figure 1c**. It was only after the formation of a monocationic complex was included that the fit was possible.

$$2\ DsH^+ + H_2PO_4^- \leftrightarrows (DsH^+)_2H_2PO_4^- \qquad (3a)$$

with the corresponding constant

$$\log K_{241} = [(DsH^+)_2H_2PO_4^-] / [DsH^+]^2[H_2PO_4^-] \qquad (3b)$$

The refined value is $\log K_{241} = 3.96 \pm 0.02$ (**Table 1**).

A further unexpected subtlety was revealed (supported by DSC measurement below): even though the K_{sp} of $DsH.H_2PO_4$(s) was lower than that of DsH.Cl(s), under the concentrations in Set 4 samples, it was the hydrochloride salt that precipitated. The solubility product of the phosphate salt was below the equilibrium constant value, partly because the phosphate was preferentially tied up with the water-soluble monocationic complex. The discussion in Sec. 3.4.2 further elaborates on this.

3.4 Desipramine solid state characterizations

3.4.1 Elemental analysis

Elemental analysis (EA) results are shown in **Tables 2 and 3**. The CHN analysis of the reference (Sigma-Aldrich) DsH.Cl(s) solid was 70.89% C, 7.46% H, 9.20% N. Evidently, the solids isolated from Set 5 (phosphate-free) from pH 1.3-7.5 suspensions are likely the *anhydrous* DsH.Cl(s) (**Table 2**).

The solids isolated from phosphate-containing suspensions (**Table 3**) have less obvious identities based on the elemental analyses. As a guide, the comment column in **Table 3** lists the species suggested from the pH-specific PXRD analyses (below). Based on theoretically-calculated CHN percentages, most of the samples appear to be extensively hydrated (or not adequately dried). Sample OM15 (pH 11.1) is compatible with Ds.2H_2O, while OM14 (pH 9.57) and OM24 (pH 9.44) are more concordant with Ds.6H_2O. The samples in the pH 3.84-8.55 interval are compatible with hydrates of the 2:1 phosphate salt: from 4-hydrate (OM12) to 16-hydrate (OM23). EA of OM21 is consistent with a dihydrate of the 1:1 phosphate salt. However, the TGA data (**Figure 2**) indicates lower levels of hydration than that of EA, although the trends between the two types of assessments are similar. The equilibrium analysis of the log *S*-pH data, consistent with the constants reported in **Table 1**, suggests that at pH 9.44 and 9.58, the only solid present in the suspension is the free base. The above suggests that the phosphate salts may have a high tendency to precipitate in mostly hydrated forms. A well-known characteristic of *drug-free* sodium phosphate salts to be highly hydrated (up to dodecahydrate) may have spilled over into drug-phosphate salts.

3.4.2 Solid state analyses of precipitates obtained at different pH

Results of DSC analyses of precipitates as well as the neat DsHCl (Sigma-Aldrich) are shown in **Figure 3**. All samples except for DsHCl and the precipitate obtained at pH 2.09 from the chloride-free solution showed broad endotherms at around 100-120°C in DSC scans (OM12, OM13, OM14, OM23, OM24, OM25, OM15, and OM21). The results of thermogravimetric analyses (TGA) presented in **Figure 2** show that the endotherms observed at 100-120°C are apparently due to the formation of hydrates since there were weight losses in the approximately similar temperature; the onset of weight loss in TGA scans was at somewhat lower temperature due to the effect of nitrogen purging during the experiments. The presence of endotherms in the DSC scans at around 100°C and the weight loss in the TGA scans at temperatures close to 100°C indicate that any moisture associated with the solid is bound, possibly, as part of the crystal lattice or embedded deep into crystal channels (*cf*., **Table 3**). The PXRD patterns of the precipitates presented in **Figure 4** indicate that all the precipitates are also crystalline, although an amorphous halo was observed in PXRD patterns in one of the two precipitates isolated at pH 11.10. As

shown by the DSC heat-cool-heat cycle of a representative sample (OM13) in **Figure 3d** that once a sample is heated beyond its dehydration endotherm, it converts to the amorphous form unless there was a separate endotherm originally present in the sample at higher temperature (see **Figures 3a** and **3b** for sample OM21).

Although the crystalline nature of the precipitates obtained from phosphate buffered solutions at different pH cannot be readily distinguished by the DSC scans as most of them have similar dehydration endotherms at around 100°C, distinct differences exist in their PXRD patterns. As shown in **Figure 4**, there are three different PXRD patterns at (a) pH 11.1, (b) pH 9.44-7.41 and (c) pH 2.13; any minor difference observed in the range of pH 9.44 to 7.41 could be due to the difference in hydration of the crystals. These three distinctly different PXRD patterns may be attributed to the existence of, respectively, (a) Ds (free base), (b) $(DsH^+)_2HPO_4^{2-}$(s) and (c) $(DsH^+)H_2PO_4^-$(s). The formation of these species agree with the ionization of phosphoric acid, which has pK_a values of 1.92, 6.70, and 11.72 (25°C, I = 0.15 M). It is evident from **Figure 3a** that the free base and $(DsH^+)_2HPO_4^{2-}$(s) exist in crystalline states only as hydrates and they convert to the amorphous phase after dehydration. On the other hand, although a hydrate, $(DsH^+)H_2PO_4^-$(s) (pH 2.13) maintains its crystallinity after dehydration (**Figure 3b**). Since the solids remain in equilibrium with water during the determination of pH versus solubility profile, these results demonstrate that the solids always remain in the crystalline state during solubility studies.

In **Figure 3a**, sample OM11 ("phosphate-poor") shows an endotherm that matches that of the reference DsHCl (Sigma-Aldrich) at 217°C. It may appear surprising that OM11, consisting of 0.14 M total phosphate concentration (**Table S2**), does not form a phosphate precipitate since $K_{sp}^{1:1} < K_{sp}^{DsH.Cl}$ (**Table 1**). There is clearly ample amount of available chloride (0.29 M) to form the drug-chloride precipitate, given that the product of $[DsH^+]$ and $[Cl^-]$ exceeds the $K_{sp}^{DsH.Cl}$ value. At pH 2.09, most of the available monohydrogen phosphate is tied up in the cationic drug-phosphate complex, $[(DsH^+)_2.H_2PO_4^-]$, whose concentrations is calculated to be 0.11 M. There is simply not enough *uncomplexed* monohydrogen phosphate available to form the drug-phosphate salt under these conditions. The DSC confirms the above equilibrium analysis.

Sample OM21 ("chloride-free" in **Figure 3a**) at pH 2.13 was prepared from the desipramine free base, so the endotherm at 175°C (the second dip in the DSC scan in **Figure 3a**) is likely that of the melting point of the 1:1 desipramine phosphate salt. **Figure 3b** shows the heat-cool-heat cycle, where the first endotherm disappears, and a sharpened dip at the higher temperature persists, suggesting a dehydration process of the 1:1 phosphate salt.

In samples OM12 and OM22 (pH 3.9), the monoanionic phosphate is near that of the total phosphate concentration, so the expected solid should not contain any chloride salt, based on the

equilibrium analysis. The transition pH from (DsH).H_2PO_4(s) to $(DsH)_2$.HPO_4(s) is estimated to be at pH_{max} between 4.0 (**Figures 1a**, and **1b**) and 4.7 (upper curve in **Figure 1c**), depending on total concentrations used. The DSC scan of one of these samples isolated at pH 3.9 (OM12) in **Figure 3a** show only the dehydration endotherm around 100°C indicating hydrate formation, and when the heat-cool-cycle was conducted, the material converted to amorphous upon dehydration (**Figure 3c**). In this respect, the sample OM12 behaves like OM13 (pH 7.4) (**Figure 3d**), which has been attributed to the formation of a 2:1 phosphate salt. Since the DSC scan of OM12 differs from that of OM21, which, as mentioned later, is considered to be a 1:1 phosphate salt, it is very likely that a 2:1 phosphate salt was formed from the buffered solution at pH 3.9. The similarity in crystal patterns between Samples OM12 and OM13 could, however, not be confirmed by PXRD as the isolated sample of OM12 was insufficient to run a PXRD experiment.

It may be noted in **Figure 4** that PXRD patterns of two precipitates isolated at pH 11.1 differ considerably with respect to their degree of crystallinity, one showing larger amorphous halo than the other. Although we are not aware of any previous study of the solid state properties of desipramine free base, they could be similar to physicochemical attributes of a related compound, chlorpromazine free base, which is known to be amorphous in the solid state (Zografi and Zarenda, 1966). It is evident in **Figure 4** that the material isolated from aqueous medium at pH 11.1 is a crystalline hydrate that can readily convert to the amorphous form during preparation (hence the difference in amorphous halo) or upon heating. It may also be noted from the TGA scans in **Figure 2** that the free base is volatile as the sample continues losing weight after dehydration.

In contrast to precipitates isolated from the phosphate-buffered solutions, the sample OM11 (pH 2.09) that was isolated from the phosphate-poor solution showed a melting endotherm only at 217^{o}C, indicative of the formation of anhydrous DsH.Cl, which is precisely what was predicted from the refinement of log *S*-pH data in Set 4. On the other hand, the chloride-free OM21 (pH 2.13) showed two melting endotherms; one around 100^{o}C and other around 175^{o}C. This is indicative of the 1:1 phosphate salt showing a dehydration pattern. Once the sample was subjected to heat-cool-reheat cycle by first heating the sample to 120°C for dehydration, the first endotherm disappears and the second endotherm due to the melting of the sample becomes even sharper, indicating the high crystallinity of the 1:1 drug-phosphate salt **(Figure 3b).**

The elemental analysis of phosphate containing preparations shown in **Table 3** and the TGA scans of the same in **Figure 2** show that there were different amounts of water present in different samples. As mentioned under **Materials and methods**, the samples were only air-dried before analysis. No further treatment was done to maintain the sample closely similar to what were present in equilibria

with aqueous media. However, it is possible that all samples did not dry to the same extent during air-drying depending on how much solid was present in a wet mass and how long it was dried. Although the difference in water content did not change the nature of DSC scans and the powder X-ray patterns, it could be responsible for the observed difference in moisture content in elemental analysis and TGA scans. To investigate this possibility, we subjected samples OM13 (7.41) and OM23 (pH 8.03) that showed, respectively, 5.3 and 25.7% weight loss, to identical humidity conditions of 50% RH at 25°C by using a VTI SA dynamic vapor sorption instrument (TA Instruments, Wilmington, DE) for equilibration until there was no weight gain or loss due to moisture sorption or desorption. As shown in **Figure S1** (Supplementary Materials), there was ~2% moisture sorption by OM13 (**Figure S1c**), while there was a moisture desorption of ~17% with OM23 (**Figures S1a**). TGA scans of the samples equilibrated at 25°C/50% RH showed the weight loss of both samples were similar and in the range of 5-6% (**Figures S1b** and **S1d**), corresponding to approximately 2 moles of water. Thus, it is evident that the difference in moisture contents observed in **Table 3** and **Figure 2** could be due to the difference in the extent of drying. However, DSC scans and PXRD patterns of various samples show that any difference in moisture content did not change crystalline nature of the precipitates formed in equilibria with phosphate buffers, and, as evident from the representative examples in **Figures 3c** and **3d**, irrespective of the extent of hydration, any $(DsH^+)_2HPO_4^{2-}$hydrates formed may convert to amorphous form upon dehydration by heating.

4. Conclusions

The critical analysis of the desipramine system in saturated aqueous saline phosphate buffer suspensions revealed complexity not addressed previously.

While most pH versus solubility studies of free bases are conducted by adjusting pH by using a monoprotic acid like HCl, a triprotic acid H_3PO_4 was used in the present study to determine the solubility-pH profile of 1:1 desipramine phosphate salt. The results are compared with the solubility-pH profile of the 1:1 desipramine chloride salt determined in a phosphate-free medium. The results showed the complex nature of the solid phase formed under different pH conditions in the phosphate buffer. At pH 11, the crystalline hydrate of the desipramine free base was formed and existed as the solid phase. At lower pH in the range of 4 to 9.5, the solid species in equilibria with solutions was crystalline $(DsH^+)_2HPO_4^{2-}$(s) hydrate, and at the lower pH of 2.1, the solid phase was the hydrated $(DsH^+)H_2PO_4^-$(s). These three solid phases were distinct from each other; while both the crystalline free base and the $(DsH^+)_2HPO_4^{2-}$hydrates converted to the amorphous phase upon dehydration by heating, the hydrated $(DsH^+)H_2PO_4^-$(s) remained crystalline upon dehydration. The different solid phases present in equilibia with solutions influenced solubility vs. pH of desipramine hydrochloride in phosphate buffers. They are

also responsible for the difference between solubility profile of desipramine hydrochloride in phosphate buffers from that in the phosphate-free medium.

Given the solid state characterization in the present study, it is now clear that the earlier interpretation by Avdeef (2014b) of the desipramine hydrochloride behavior in 0.15 M phosphate buffer (Bergström *et al*., 2004) was based on an invalid assumption that the precipitate in the pH 7-9 region was the desipramine free base. It is now clear that the free base exists only above pH 9.5 in the phosphate buffer.

Acknowledgements

This work was supported by Ministry of Education, Science and Technological Development of Serbia [grant numbers 172035, 172008). The authors gratefully acknowledge Petnica Science Center, Serbia, for the HPLC analysis. The authors thank Ms. Nitprapa Siriwannakij and Ms. Nirali Patel of College of Pharmacy and Health Sciences, St. John's University, Queens, NY, for technical assistance with solid state characterization of samples.

Appendix - Example of an explicit mass action model

The following equilibrium reactions are characteristic of much of the titration data in the study. As a generalized example of a monoprotic weak base, B, a saturated solution can be defined by the equations (4 homogeneous and 4 heterogeneous phases) and the corresponding constants:

$$BH^+ \leftrightarrows H^+ + B \qquad K_a = [H^+][B] / [BH^+] \qquad (A.1)$$

$$H_3PO_4 \leftrightarrows H^+ + H_2PO_4^- \qquad K_{a1}^{buf} = [H^+]\,[H_2PO_4^-] / [H_3PO_4] \qquad (A.2)$$

$$H_2PO_4^- \leftrightarrows H^+ + HPO_4^{2-} \qquad K_{a2}^{buf} = [H^+]\,[HPO_4^{2-}] / [H_2PO_4^-] \qquad (A.3)$$

$$HPO_4^{2-} \leftrightarrows H^+ + PO_4^{3-} \qquad K_{a3}^{buf} = [H^+]\,[PO_4^{3-}] / [HPO_4^{2-}] \qquad (A.4)$$

$$B(s) \leftrightarrows B \qquad S_0 = [B] \qquad (A.5)$$

$$(BH^+)_2 \cdot HPO_4^{2-}(s) \leftrightarrows 2\,BH^+ + HPO_4^{2-} \qquad K_{sp}^{2:1} = [BH^+]^2\,[HPO_4^{2-}] \qquad (A.6)$$

$$BH^+ \cdot H_2PO_4^-(s) \leftrightarrows BH^+ + H_2PO_4^- \qquad K_{sp}^{1:1} = [BH^+]\,[H_2PO_4^-] \qquad (A.7)$$

$$BH^+ \cdot Cl^-(s) \leftrightarrows BH^+ + Cl^- \qquad K_{sp}^{BH.Cl} = [BH^+]\,[Cl^-] \qquad (A.8)$$

If the concentration of the drug is kept below its intrinsic solubility, then usually Eqs. (A.5)-(A.8) need not be considered. In such a homogeneous solution, the three independent reactants are B, PO_4^{3-} and H^+. The corresponding mass balance equations may be stated as

$$[B]_{tot} = [B] + [BH^+] \qquad (A.9)$$

$$[PO_4]_{tot} = [PO_4^{3-}] + [HPO_4^{2-}] + [H_2PO_4^-] + [H_3PO_4] \qquad (A.10)$$

$$[H]_{tot} = [H^+] - K_w / [H^+] + [BH^+] + [HPO_4^{2-}] + 2[H_2PO_4^-] + 3[H_3PO_4] \qquad (A.11)$$

K_w is the ionization constant of water. On substituting the equilibrium quotients from Eqs. (A.1)-(A.4) into the mass balance equations, one gets three polynomials as a function of the three reactants (B, PO_4^{3-}, H^+) and the equilibrium constants K_a, K_{a1}^{buf}, K_{a2}^{buf}, K_a^{buf}, and K_w.

$$[B]_{tot} = [B] + [B][H^+]/K_a \qquad (A.12)$$

$$[PO_4]_{tot} = [PO_4^{3-}]\,\{1 + [H^+] / K_{a3}^{buf} + [H^+]^2 / K_{a3}^{buf} \cdot K_{a2}^{buf} + [H^+]^3 / K_{a3}^{buf} \cdot K_{a2}^{buf} \cdot K_{a1}^{buf}\} \qquad (A.13)$$

$$[H]_{tot} = [H^+] - K_w / [H^+] + [B][H^+]/K_a$$
$$+ [PO_4^{3-}] \{ [H^+] / K_{a3}^{buf} + 2 [H^+]^2 / K_{a3}^{buf} \cdot K_{a2}^{buf} + 3 [H^+]^3 / K_{a3}^{buf} \cdot K_{a2}^{buf} \cdot K_{a1}^{buf} \} \quad (A.14)$$

The [B], $[PO_4^{3-}]$, and $[H^+]$ roots of the above equations are solved using standard mathematical techniques (Avdeef, 2012). K_w and the ionization constants are generally provided as fixed parameters in the calculation. Those of standard buffers are coded internally, adjusted to the assay conditions of temperature and ionic strength.

If the concentration of the drug is above the intrinsic solubility and the pH of the solution is very alkaline, then Eq. (A.5) needs to be introduced into the calculation. The calculation becomes more complex, since one of the reactants loses its independence, and needs to be expressed in terms of the remaining reactants. One less mass balance equation needs to be explicitly considered in the solution for the roots. This procedure has been described in detail elsewhere (Avdeef, 2017).

If the solubility measurements are carried out in an acidic solution, with enough compound added that the solubility products $[BH^+]^2 [HPO_4^{2-}]$ and/or $[BH^+] [H_2PO_4^-]$ are exceeded, then Eqs. (A.6) and (A.7) would need to be considered in the further more complicated procedure. At very low pH, the possible role of the drug-chloride precipitate (Eq. A.8) is tested for. The program automatically checks to see if the solubility products are exceeded at a particular pH, and appropriate constraints are automatically applied. At any given pH, the program tests for any violations of the Gibbs Phase Rule. All such complicated equations are sorted out implicitly in the mass action algorithm of *p*DISOL-X, and their explicit derivations are not necessary for the computation.

References

Attwood, D., Florence, A.T, Gillan, J.M.N., 1974. Micellar properties of drugs: properties of micellar aggregates of phenothiazines and their aqueous solutions. J. Pharm. Sci. 63, 988-993.

Attwood, D., Boitard, E., Dubès, J.-P., Tachoire , H., 1997. Calorimetric study of the influence of electrolyte on the micellization of phenothiazine drugs in aqueous solution. J. Phys. Chem. B 101, 9586-9592.

Avdeef, A., Bucher, J.J., 1978. Accurate measurements of the concentration of hydrogen ions with a glass electrode: calibrations using the Prideaux and other universal buffer solutions and a computer-controlled automatic titrator. Anal. Chem. 50, 2137-2142.

Avdeef, A., 1992. pH-metric log P. 2. Refinement of partition coefficients and ionization constants of multiprotic substances. J. Pharm. Sci. 82, 183-190.

Avdeef, A., Berger, C.M., Brownell, C., 2000. pH-metric solubility. 2. Correlation between the acid-base titration and the saturation shake-flask solubility-pH methods. Pharm. Res. 17, 85-89.

Avdeef, A., 2007. Solubility of sparingly-soluble drugs. Adv. Drug Deliv. Rev. 59, 568-590.

Avdeef, A., 2012. Absorption and Drug Development Second Edition, Wiley-Interscience, Hoboken NJ.

Avdeef, A., 2014a. Anomalous solubility behavior of several acidic drugs. ADMET&DMPK 2, 33-42.

Avdeef, A., 2014b. Phosphate precipitates and water-soluble aggregates in re-examined solubility-pH data of twenty-five basic drugs. ADMET&DMPK 2, 43-55.

Avdeef, A., 2015. Suggested improvements for measurement of equilibrium solubility-pH of ionizable drugs. ADMET&DMPK 3, 84-109.

Avdeef, A., Fuguet, E., Llinàs, A., Ràfols, C., Bosch, E., Völgyi, G., Verbić, T., Boldyreva, E., Takács-Novák, K., 2016. Equilibrium solubility measurement of ionizable drugs-consensus recommendations for improving data quality, ADMET&DMPK 4, 117-178.

Avdeef, A., 2017. Cocrystal solubility product analysis – dual concentration-pH mass action model not dependent on explicit solubility equations. Eur. J. Pharm. Sci. 110, 2-18.

Bergström, C.A.S., Strafford, M., Lazarova, L., Avdeef, A., Luthman, K., Artursson, P., 2003. Absorption classification of oral drugs based on molecular surface properties. J. Med. Chem. 46, 558-570.

Bergström, C.A.S., Luthman, K., Artursson, P., 2004. Accuracy of calculated pH-dependent aqueous drug solubility, Eur. J. Pharm. Sci. 22, 387-398.

Bogardus, J.B., Blackwood, R.K. Jr., 1979. Solubility of doxycycline in aqueous solution. J. Pharm. Sci. 68, 188-194.

Bradley, J.-C., Williams, A., Lang A. Jean-Claude Bradley Open Melting Point Dataset - Version 2. http://www.chemspider.com/DatasourceDetails.aspx?id=800, accessed 12 Feb 2018.

Brunton, L., Chabner, B.; Knollman, B., 2010. Goodman and Gilman's - The Pharmacological Basis of Therapeutics (12th ed.). New York: McGraw-Hill Professional.

Butcher, G., Comer, J., Avdeef, A., 2015. pK_a-critical Interpretations of solubility–pH profiles: PG-300995 and NSC-639829 case studies. ADMET&DMPK 3, 131-140.

Fini, A., Fazio, G., Feroci, G., 1995. Solubility and solubilization properties of non-steroidal antiinflammatory drugs. Int. J. Pharm. 126, 95-102.

Florence, A.T., Parfitt, R.T., 1971. Micelle formation by some phenothiazine derivatives. II. Nuclear magnetic resonance studies in deuterium oxide. J. Phys. Chem. 76, 3554-3560.

Gebauer, D., Kellermeier, M., Gale, J.D., Bergström, L., Cölfen, H., 2014. Pre-nucleation clusters as solute precursors in crystallization. Chem. Soc. Rev., 2014, 43, 2348-2371.

Green, A.L., 1967. Ionization constants and water solubilities of some aminoalkylphenothiazine tranquilizers and related compounds. J Pharm Pharmacol. 19, 10-16.

Higuchi, T., Gupta, M., Busse, L.W., 1953. Influence of electrolytes, pH, and alcohol concentration on the solubilities of acidic drugs. J. Amer. Pharm. Assoc. (Sci. Ed.) 42, 157-161.

Janowsky, D.S., Byerley, B., 1984. Desipramine: an overview. J Clin Psychiatry. 45, 3-9.

Jaszczyszyn, A., Gąsiorowski, K., Świątek, P., Malinka, W., Cieślik-Boczula, K., Petrus, J., Czarnik-Matusewicz, B., 2012. Chemical structure of phenothiazines and their biological activity. Pharmacol. Reports 64, 16-23.

Ledwidge, M.T., Corrigan, O.I., 1998. Effects of surface active characteristics and solid state forms on the pH solubility profiles of drug-salt systems, Int. J. Pharm. 174, 187-200.

Liu, S.-T., Hurwitz, A., 1977. The effect of micelle formation on solubility and pK_a determination of acetylpromazine maleate. J. Colloid Int. Sci. 60, 410-413.

Ohlow, M.J., Moosmann, B., 2011. Phenothiazine: the seven lives of pharmacology's first lead structure. Drug Discov. Today. 16, 119-131.

Patrick, G.L., 1995. An Introduction to Medicinal Chemistry. Oxford University Press, Oxford, UK.

Pobudkowska, A., Ràfols, C., Subirats, X., Bosch, E., Avdeef, A., 2016. Phenothiazines solution complexity – determination of pK_a and solubility-pH profiles exhibiting sub-micellar aggregation at 25 and 37 ^{o}C. Eur. J. Pharm. Sci. 93, 163-176.

Serajuddin, A.T.M., Rosoff, M, 1984. pH-solubility profile of papaverine hydrochloride and its relationship to the dissolution rate of sustained-release pellets. J. Pharm. Sci. 73, 1203-1208.

Serajuddin, A.T.M., Jarowski, C.I., 1985. Effect of diffusion layer pH and solubility on the dissolution rate of pharmaceutical bases and their hydrochloride salts. I: phenazopyridine. J. Pharm. Sci. 74, 142-147.

Shoghi, E., Fuguet, E., Bosch, E., Ràfols, C., 2013. Solubility–pH profiles of some acidic, basic and amphoteric drugs. Eur. J. Pharm. Sci. 48, 291-300.

Sorby, D.L., Plein E.M., Benmaman, J.D., 1966. Adsorption of phenothiazine derivatives by solid adsorbents. J. Pharm. Sci. 55, 785-794.

Takács-Novák, K., Urac, M., Horváth, P., Völgyi, G., Anderson, B.D., Avdeef, A., 2017. Equilibrium solubility measurement of compounds with low dissolution rate by Higuchi's Facilitated Dissolution Method. A validation study. Eur. J. Pharm. Sci. 106, 133-141.

Völgyi, G., Baka, E., Box, K.J., Comer, J.E., Takács-Novák, K., 2010. Study of pH-dependent solubility of organic bases. Revisit of Henderson-Hasselbalch relationship. Anal. Chim. Acta 673, 40-46.

Völgyi, G., Marosi, A., Takács-Novák, K., Avdeef, A., 2013. Salt Solubility Products of Diprenorphine Hydrochloride, Codeine and Lidocaine Hydrochlorides and Phosphates – Novel Method of Data Analysis Not Dependent on Explicit Solubility Equations. ADMET&DMPK 1, 48-62.

Zhu, C., Streng, W.H., 1996. Investigation of drug self-association in aqueous solution using calorimetry, conductivity, and osmometry. Int. J. Pharm. 130, 159-168.

Zografi, G., Auslander, D.E., Lytell, P.L., 1964. Interfacial properties of phenothiazine derivatives. J. Pharm. Sci. 53, 573-574.

Zografi, G., Zarenda, I., 1966. The surface activity of phenothiazine derivatives at the air-solution interface. Biochem. Pharmacol. 15, 591-598.

Figure Captions

Figure 1 – Solubility-pH profiles for the desipramine at 25°C. The dashed curves were calculated with the Henderson-Hasselbalch equation, using the independently-determined pK_a = 10.28 and the intrinsic solubility log S_0 = -3.85, determined from Set 5 (*cf*., **Table 4**). The solid lines are best-fit refinement curves through the measured log *S*-pH points. (a) Sets 1 and 2 are replicate titrations, where alkaline suspensions (pH 11.6) containing $[Ds]_{tot}$ = $[Cl]_{tot}$ = 27 mM and $[PO_4]_{tot}$ = 119 mM, were acidified with HCl. No precipitate was observed below pH 4. **(b)** Set 3 represents the titration in the opposite direction, where acidified (pH 1.90) solutions, with slightly higher concentrations $[Ds]_{tot}$ = 76 mM, $[Cl]_{tot}$ = 142 mM, and $[PO_4]_{tot}$ = 140 mM, were titrated with NaOH up to pH 11.6. Precipitate appeared only above pH 4. **(c)** Set 4 (upper solid curve) was designed in order to induce precipitation of solid for pH < 4. Higher drug concentrations were used: $[Ds]_{tot}$ = $[Cl]_{tot}$ = 320 mM and $[PO_4]_{tot}$ = 150 mM. Set 5 (lower curve) consisted of buffer-free 0.15 M NaCl suspensions of DsHCl, with HCl/NaOH to adjust the pH. The data in Set 5 were used to determine the drug-hydrochloride solubility product in phosphate-free suspensions, and to determine the intrinsic solubility, log S_0, in the absence of phosphate complexation.

Figure 2 – Thermogravimetric analysis (TGA) scans of precipitates obtained at different pH. Samples were used 'as is' and the moisture loss could vary depending on how the samples were isolated and dried. While the weight loss equilibrated after dehydration of samples obtained at pH 2.13, 7.41, and 8.03 (relatively flat region >100°C), the weight loss continued in pH 9.44, 9.47 and 11.10 samples, possibly due to both dehydration and sublimation of materials. Temperatures at relatively flat regions were used to calculate weight losses in different scans.

Figure 3 – Differential scanning calorimetric (DSC) scans of different precipitates isolated during the determination of solubility-pH profile of desipramine HCl. (**a)** DSC scans of precipitates and the neat desipramine HCl ('as is') as a function of temperature, indication dehydration endotherms around 100°C and melting endotherms at higher temperature; (**b**) heat-cool-heat run cycles of precipitate isolated at pH 2.13 (OM21), indicating dehydration in cycle 1 and only the melting peak and no dehydration during reheating in cycle 3; (**c**) heat-cool-heat run cycles of precipitate isolated at pH 3.86 (OM12), indicating dehydration in cycle 1 and no dehydration or melting peaks during reheating in cycle 3; and (**d**) heat-cool-heat run cycles of precipitate isolated at pH 7.41 (OM13), indicating dehydration in cycle 1 and no dehydration or melting peaks during reheating in cycle 3.

Figure 4 – Powder X-ray diffraction (PXRD) patterns of precipitates isolated at different pH.

Table 1. Refinement of desipramine equilibrium constants [a]

Set and/or Sample	log S_0	SD	log $K_{sp}^{1:1}$ [DsH^+][$H_2PO_4^-$]	SD	log $K_{sp}^{2:1}$ [DsH^+]^2[HPO_4^{2-}]	SD	log K_{241} [$(DsH^+)_2.H_2PO_4^-$]	SD	log K_{221} [$DsH^+.Ds.HPO_4^{2-}$]	SD	log $K_{sp}^{1:1}$ [DsH^+][Cl^-]	SD	pH_{range}	pH_{max}	I_{avg} [b]	GOF [c]	N [c]
1 & 2	-3.85	n.v.			-7.38	0.01			4.58	0.10			4.4-11.6	9.5	0.41	0.51	26
OM21			-2.55	n.d.[d]	-7.38	n.r.[e]							2.1	3.3	0.15	n.d.[d]	1
3 & OM14, OM15, OM24, OM25	-3.85	n.v.			-7.06	0.03			4.80	0.10			4.0-11.5	9.3	0.41	0.67	15
OM23			-2.55	n.r.[e]	-7.27	n.d.[d]							8.0	4.9	0.28	n.d.[d]	1
4 & OM22			-2.55	n.r.[e]	-7.06	n.r.[e]	3.96	0.02			-2.19	n.r.[e]	2.0-3.8	4.7	0.30	0.37	4
5	-3.85	0.04									-2.19	0.03	1.3-10.0	8.0	0.25	0.50	7

[a] 25°C. Ref. ionic str.=0.15 M. pK_a=10.28 in all cases. Max. buffer capacity=49 to 137 mM/pH in the data. Determined constant underlined. See text for other terms.

[b] Average ionic strength (M).

[c] Goodness-of-fit=$\{1/(N-N_r)\ \Sigma\ [(\log S^{obs}-\log S^{calc})/SD(\log S)]^2\}^{1/2}$: SD(log S)=0.10 assumed for all points; N=no. of log S points used; N_r=no. of varied parameters.

[d] n.d.=not defined, since N=1.

[e] n.r.=included in the model, but not refined.

Table 2. Elemental analyses of solids isolated from Set 5 (phosphate-free)

Sample	pH	%C	%H	%N
1	1.31	70.18	7.25	9.12
2	2.38	70.62	7.64	9.34
3	3.02	70.53	7.22	9.25
4	4.93	70.96	7.29	9.21
5[a]	7.59	70.85	7.30	9.18

[a] Suspension appeared to be supersaturated.

Table 3. Elemental analyses of solids isolated from phosphate-containing preparations

Sample	pH	%C	%H	%N	Comment[a]	x.H_2O(EA)[b]	x.H_2O(TGA)[c]
OM11	2.09	76.64	10.36	9.88			
OM21[d]	2.13	54.65	7.25	7.03	DsH.H_2PO_4(s)	2	0.7
OM22	3.84	57.51	6.95	7.36		7	
OM12	3.86	62.12	8.13	7.97		4	
2 (Set 2)	5.36	60.94	7.52	8.16		5	
OM13	7.41	60.41	7.80	7.82	$(DsH)_2$.HPO_4(s)	5	2
5 (Set 2)	7.50	60.78	7.36	7.87		5	
OM23	8.03	46.80	8.44	6.01	$(DsH)_2$.HPO_4(s)	16	9
6 (Set 1)	8.55	58.70	7.20	7.73		7	
OM24	9.44	58.49	8.37	7.66	Ds(s)	6	0.6
OM14	9.57	56.64	6.46	7.29	Ds(s)	6	0.7
OM15	11.10	72.47	9.09	9.36	Ds(s)[e]	2	0.5

[a] Species suggested from PXRD, accounting for the solution pH from which the solid was isolated (*cf.*, **Figure 4**).

[b] Estimated number of water molecules in analyzed solid, based on theoretical CHN values.

[c] Estimated number of water molecules in analyzed solid, based on TGA analysis (*cf.*, **Figure 2**).

[d] Chloride-free.

[e] Mixture of crystalline and amorphous material.

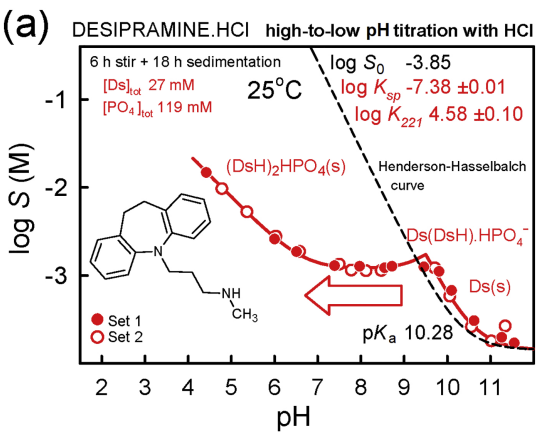
(a)
DESIPRAMINE.HCl high-to-low pH titration with HCl
6 h stir + 18 h sedimentation
[Ds]tot 27 mM
[PO4]tot 119 mM
25°C
log S0 -3.85
log Ksp -7.38 ±0.01
log K221 4.58 ±0.10
(DsH)2HPO4(s)
Henderson-Hasselbalch curve
Ds(DsH).HPO4-
Ds(s)
pKa 10.28
Set 1
Set 2
log S (M)
pH

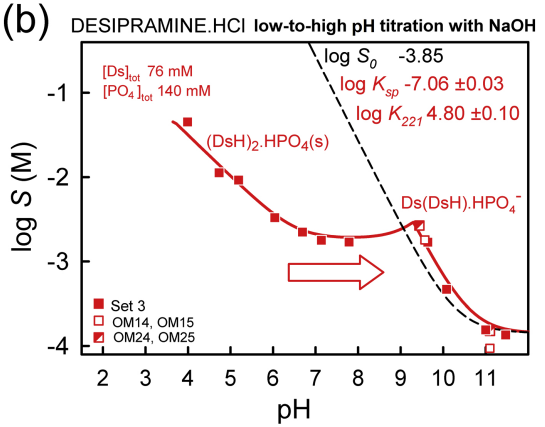
(b)
DESIPRAMINE.HCl low-to-high pH titration with NaOH
[Ds]tot 76 mM
[PO4]tot 140 mM
log S0 -3.85
log Ksp -7.06 ±0.03
log K221 4.80 ±0.10
(DsH)2.HPO4(s)
Ds(DsH).HPO4-
Set 3
OM14, OM15
OM24, OM25
log S (M)
pH

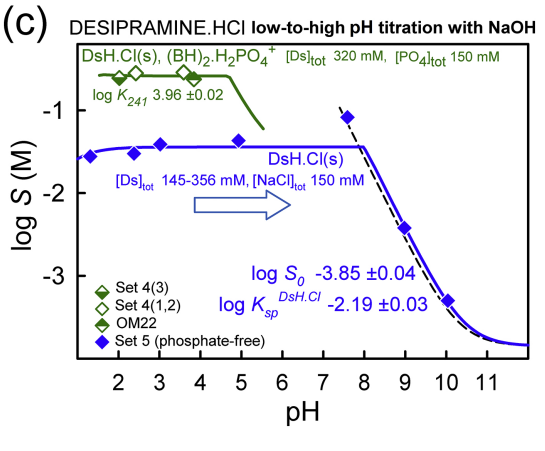
(c)
DESIPRAMINE.HCl low-to-high pH titration with NaOH
DsH.Cl(s), (BH)2.H2PO4+ [Ds]tot 320 mM, [PO4]tot 150 mM
log K241 3.96 ±0.02
DsH.Cl(s)
[Ds]tot 145-356 mM, [NaCl]tot 150 mM
log S0 -3.85 ±0.04
log Ksp DsH.Cl -2.19 ±0.03
Set 4(3)
Set 4(1,2)
OM22
Set 5 (phosphate-free)
log S (M)
pH

Figure 1

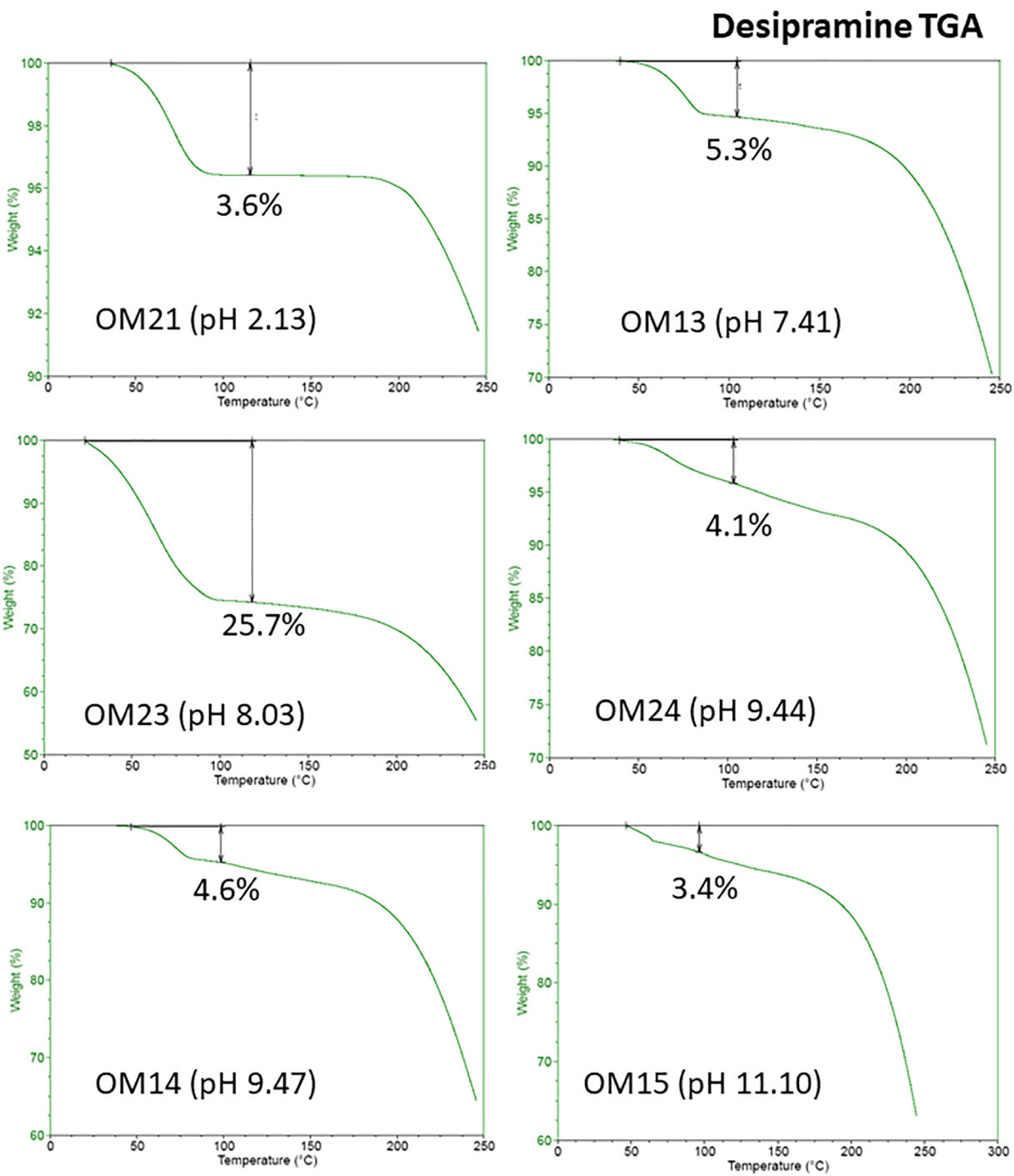
Desipramine TGA
3.6%
OM21 (pH 2.13)
5.3%
OM13 (pH 7.41)
25.7%
OM23 (pH 8.03)
4.1%
OM24 (pH 9.44)
4.6%
OM14 (pH 9.47)
3.4%
OM15 (pH 11.10)
Weight (%)
Temperature (°C)

Figure 2

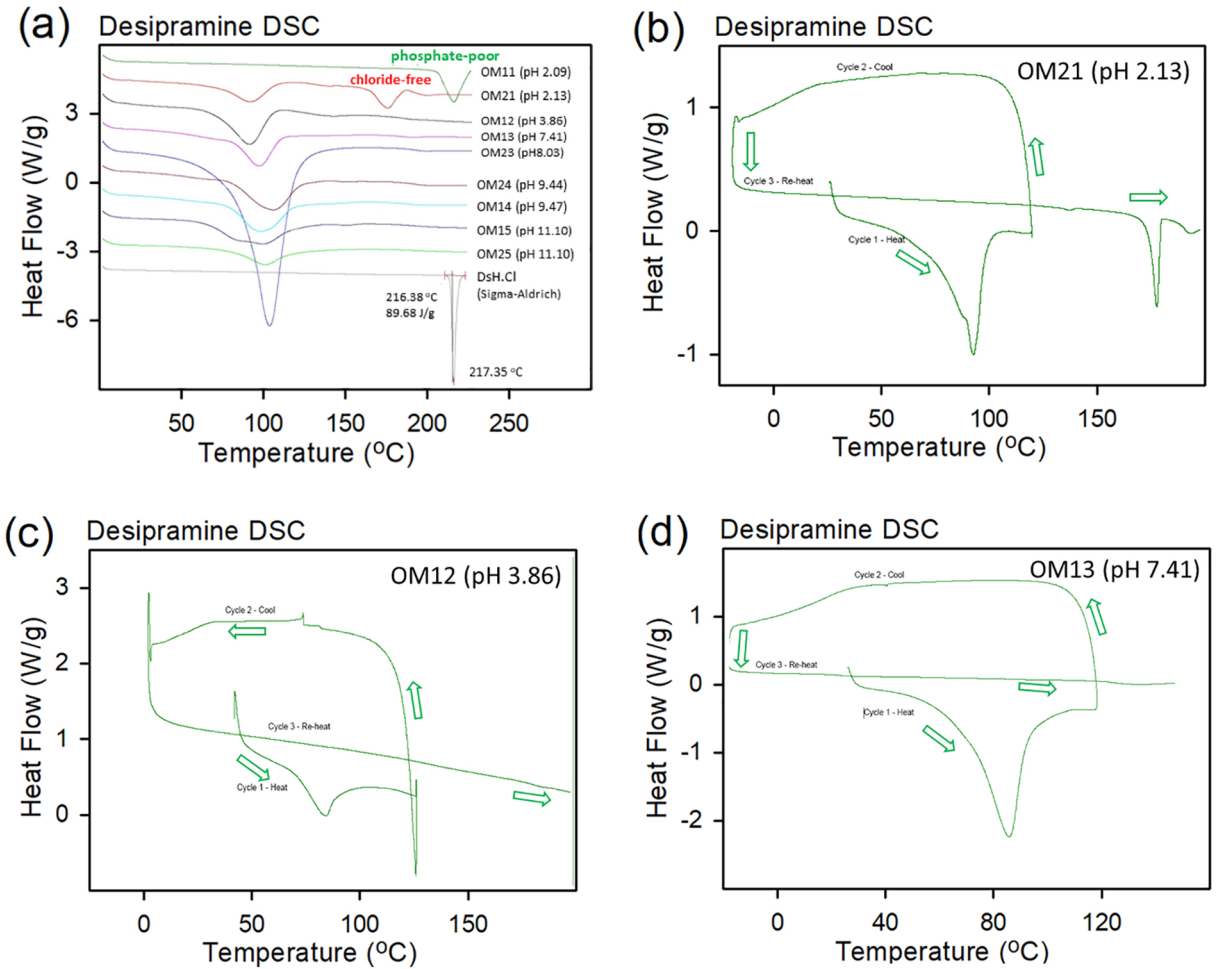
(a)
Desipramine DSC
phosphate-poor
chloride-free
OM11 (pH 2.09)
OM21 (pH 2.13)
OM12 (pH 3.86)
OM13 (pH 7.41)
OM23 (pH8.03)
OM24 (pH 9.44)
OM14 (pH 9.47)
OM15 (pH 11.10)
OM25 (pH 11.10)
DsH.Cl
(Sigma-Aldrich)
216.38 °C
89.68 J/g
217.35 °C
Heat Flow (W/g)
Temperature (°C)
(b)
Desipramine DSC
OM21 (pH 2.13)
Cycle 2 - Cool
Cycle 3 - Re-heat
Cycle 1 - Heat
Heat Flow (W/g)
Temperature (°C)
(c)
Desipramine DSC
OM12 (pH 3.86)
Cycle 2 - Cool
Cycle 3 - Re-heat
Cycle 1 - Heat
Heat Flow (W/g)
Temperature (°C)
(d)
Desipramine DSC
OM13 (pH 7.41)
Cycle 2 - Cool
Cycle 3 - Re-heat
Cycle 1 - Heat
Heat Flow (W/g)
Temperature (°C)

Figure 3

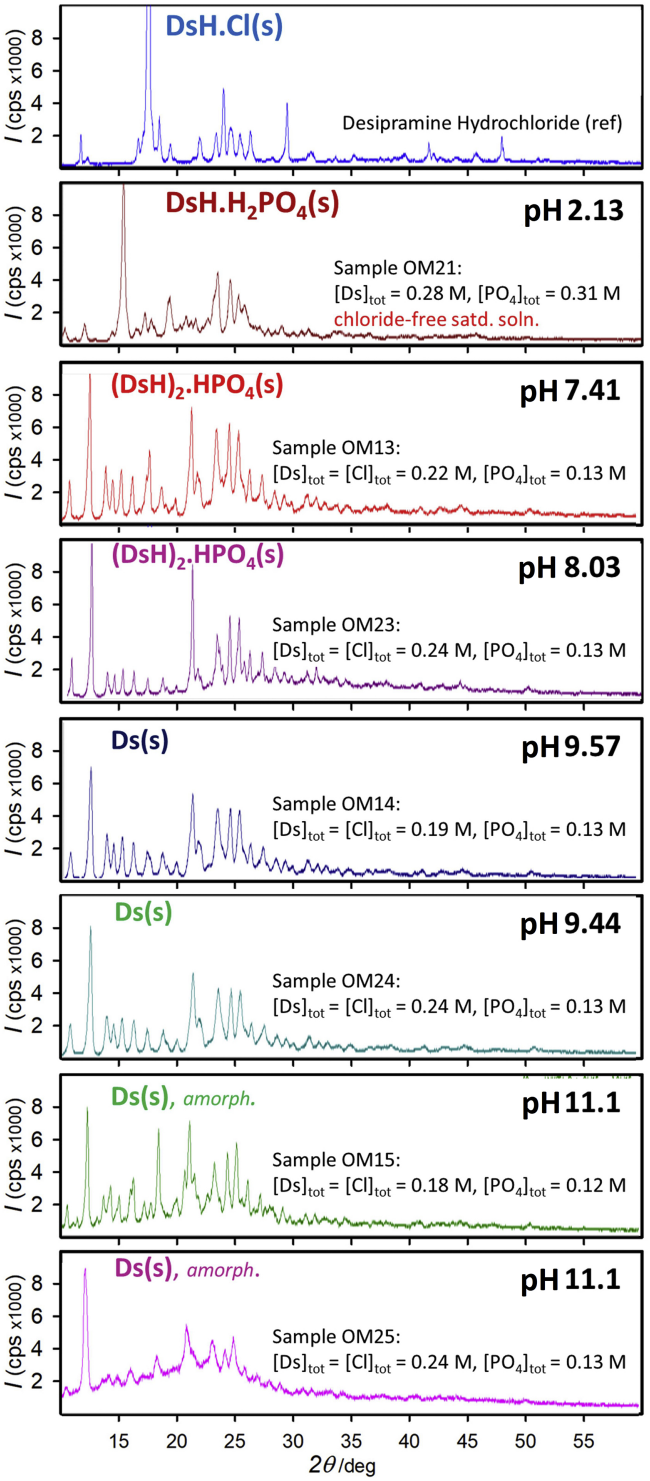
DsH.Cl(s)
Desipramine Hydrochloride (ref)
DsH.H2PO4(s)
pH 2.13
Sample OM21:
[Ds]tot = 0.28 M, [PO4]tot = 0.31 M
chloride-free satd. soln.
(DsH)2.HPO4(s)
pH 7.41
Sample OM13:
[Ds]tot = [Cl]tot = 0.22 M, [PO4]tot = 0.13 M
(DsH)2.HPO4(s)
pH 8.03
Sample OM23:
[Ds]tot = [Cl]tot = 0.24 M, [PO4]tot = 0.13 M
Ds(s)
pH 9.57
Sample OM14:
[Ds]tot = [Cl]tot = 0.19 M, [PO4]tot = 0.13 M
Ds(s)
pH 9.44
Sample OM24:
[Ds]tot = [Cl]tot = 0.24 M, [PO4]tot = 0.13 M
Ds(s), amorph.
pH 11.1
Sample OM15:
[Ds]tot = [Cl]tot = 0.18 M, [PO4]tot = 0.12 M
Ds(s), amorph.
pH 11.1
Sample OM25:
[Ds]tot = [Cl]tot = 0.24 M, [PO4]tot = 0.13 M
I (cps x1000)
2θ/deg

Figure 4